

Asymmetric Explosions of Thermonuclear Supernovae

C. R. Ghezzi^{1 2 *}, E. M. de Gouveia Dal Pino² and J. E. Horvath²

¹*Departamento de Matemática, Instituto de Matemática, Estatística e Computação Científica, Universidade Estadual de Campinas, 13081-970, Campinas, SP, Brasil.*

²*Instituto de Astronomia, Geofísica e Ciências Atmosféricas, Universidade de São Paulo, R. do Matão, 1226, Cd. Universitária, 05508-090, São Paulo, SP, Brasil*

ABSTRACT

A type Ia supernova explosion starts in a white dwarf as a laminar deflagration at the center of the star and soon several hydrodynamic instabilities (in particular, the Rayleigh-Taylor (R-T) instability) begin to act. In previous work (Ghezzi, de Gouveia Dal Pino, & Horvath 2001), we addressed the propagation of an initially laminar thermonuclear flame in presence of a magnetic field assumed to be dipolar. We were able to show that, within the framework of a fractal model for the flame velocity, the front is affected by the field through the quenching of the R-T instability growth in the direction perpendicular to the field lines. As a consequence, an *asymmetry* develops between the magnetic polar and the equatorial axis that gives a prolate shape to the burning front. We have here computed numerically the total integrated asymmetry as the flame front propagates outward through the expanding shells of decreasing density of the magnetized white dwarf progenitor, for several chemical compositions, and found that a total asymmetry of about 50% is produced between the polar and equatorial directions for progenitors with a surface magnetic field $B \sim 5 \times 10^7$ G, and a composition $^{12}\text{C} = 0.2$ and $^{16}\text{O} = 0.8$ (in this case, the R-T instability saturates at scales ~ 20 times the width of the flame front). This asymmetry is in good agreement with the inferred asymmetries from spectropolarimetric observations of very young supernova remnants, which have recently revealed intrinsic linear polarization interpreted as evidence of an asymmetric explosion in several objects, such as SN1999by, SN1996X, and SN1997dt. Larger magnetic field strengths will produce even larger asymmetries. We have also found that for *lighter* progenitors (i.e., progenitors with smaller concentrations of ^{16}O and larger concentrations of ^{12}C) the total asymmetry is larger.

Key words: supernovae: general, white dwarfs, magnetohydrodynamics, instabilities

1 INTRODUCTION

According to the current modelling, the explosion of a type Ia supernova starts as a thermonuclear deflagration of a Chandrasekhar mass white dwarf of carbon-oxygen (C+O) or oxygen-neon-magnesium (O+Ne+Mg) compositions. Due to the action of several hydrodynamic instabilities, in particular, the Rayleigh-Taylor (R-T), the initially laminar propagation does not survive as such and the combustion front rapidly develops a complex topology. A cellular stationary combustion (followed by a turbulent combustion regime) is rapidly achieved by the flame and maintained up to the end of the so-called flamelet regime when a transition to detonation may occur. As in the case of chemical laboratory flames (Gostintsev et al 1988), thermonuclear flames prob-

ably develop a self-similar behavior due to the action of the hydrodynamic instabilities. Under this hypothesis of a self-similar deflagration regime, the effective flame speed is well described by a fractal scaling law, as previously proposed by several authors (Woosley 1990, Timmes & Woosley 1992, Niemeyer & Hillebrandt 1995, Niemeyer & Woosley 1997, see also Ghezzi, de Gouveia Dal Pino & Horvath 2001), namely

$$v_{frac} = v_{lam} \left(\frac{L_{max}}{l_{min}} \right)^{(d-2)}, \quad (1)$$

where v_{lam} is the laminar velocity (as obtained, for example, in Timmes & Woosley 1992); L_{max} and l_{min} are the maximum and minimum Rayleigh-Taylor wavelength perturbations, respectively (see Chandrasekhar 1961); and d is the fractal dimension, which may assume a range of values,

* E-mail: ghezzi@ime.unicamp.br

$2 \leq d < 3$ (Woosley 1990; see also Ghezzi, de Gouveia Dal Pino & Horvath 2001).

In a previous work (Ghezzi, de Gouveia Dal Pino & Horvath 2001, hereafter, Paper I), we addressed the propagation of an initially laminar thermonuclear flame in presence of a magnetic field assumed to be of dipolar geometry. The main result of that work was that within the framework of the fractal models for the flame velocity in the wrinkled and turbulent regimes, the front is affected by the field that inhibits the growth of the R-T instability in the direction perpendicular to the field lines. As a consequence, an *asymmetry* is established between the magnetic polar and the equatorial axis that gives a prolate shape to the burning front (see Figure 1). In that work, an estimate of the intrinsic asymmetry as a function of the field and the core density was presented and discussed in the context of type Ia supernova explosions. Nevertheless, several aspects of this problem needed to be clarified as, for instance, a computation of the total integrated asymmetry, as the burning front propagates through the outer, density-decreasing shells of the magnetized expanding progenitor star, and also its meaning for the observation of SNIa remnants. We here present the results of one-dimensional numerical calculations of the integrated asymmetry through white dwarf progenitors with different initial chemical compositions, taking into account the expansion of the star (which is assumed to be homologous).

2 INSTANTANEOUS AND CORRECTED ASYMMETRY

According to the model developed in Paper I, in the presence of a dipolar magnetic field, the ratio of the propagation velocity of the burning front in the polar and equatorial directions of the star is given by

$$A(\rho) = \frac{v_{pol}(\rho)}{v_{eq}(\rho)} = \left(1 + \frac{B^2/8\pi}{\rho v_{lam}^2/2}\right)^{d-2}, \quad (2)$$

where v_{pol} and v_{eq} are the velocities at the polar and equator directions, respectively. This equation shows that the asymmetry of the velocity field is controlled by the quotient of the magnetic pressure ($B^2/8\pi$) and the ram pressure of the gas ($\propto \rho v_{lam}^2$). We shall label $A(\rho)$ as the *instantaneous asymmetry* as a function of the density ρ for an initially spherical flame. In paper I, we have computed this quantity for different magnetic field intensities.

It is clear, however, that $A(\rho)$ will be increasingly different from the quotient above as time elapses and the flame propagates outward through the star, since the flame in both directions will be encountering decreasing densities ahead. Therefore, a full integration of the asymmetry is needed to account for this fact.

Let us first assume that the star does not expand to derive a zero-th order correction. Since the polar flame front is faster than the equatorial front, the former will encounter lower densities first. If label the difference of densities in each direction as $\Delta\rho = (\rho_{eq} - \rho_{pol}) > 0$, the polar front faces a density $\rho_{pol} = \rho - \Delta\rho$ when the equatorial front is at $\rho_{eq} = \rho$. To this order, a *corrected asymmetry* (which takes

into account the deformation of the flame) may be defined by

$$\tilde{A}(\rho) = \frac{v_{pol}(\rho - \Delta\rho)}{v_{eq}(\rho)}. \quad (3)$$

Since the fractal propagation velocity is a continuous and differentiable function of the density, we can expand v_{pol} in a Taylor series around ρ and keep the zeroth and first order terms provided that $\Delta\rho \ll \rho$, to yield

$$\tilde{A}(\rho) = \frac{v_{pol}(\rho) - \frac{\partial v_{pol}(\rho)}{\partial \rho} \Delta\rho}{v_{eq}(\rho)}, \quad (4)$$

which may be rearranged to display the instantaneous asymmetry and a correction term as

$$\tilde{A}(\rho) = A(\rho) - \left[\frac{1}{v_{eq}} \frac{\partial v_{pol}(\rho)}{\partial \rho} \right] \Delta\rho \equiv A(\rho) + A_c(\rho), \quad (5)$$

where

$$A_c(\rho) = - \left[\frac{1}{v_{eq}} \frac{\partial v_{pol}(\rho)}{\partial \rho} \right] \Delta\rho, \quad (6)$$

is the correction term for the asymmetry (see below).

Given that $v_{pol} > v_{eq}$ and both velocities increase with decreasing density¹, the difference between v_{pol} and v_{eq} is necessarily larger than the difference that they would have by imposing the same density ahead for both flames. In other words, the *corrected asymmetry* $\tilde{A}(\rho)$ must be larger than the instantaneous asymmetry $A(\rho)$. Moreover, the value of $A_c(\rho)$ depends on the value of $\Delta\rho$, which in turn, depends on the value of the corrected asymmetry $\tilde{A}(\rho)$ defined in Eq.(5). We may then find a solution to the non-linear Eq. (5) by discretizing and solving it iteratively²

$$\tilde{A}_n(\rho) = A_{n-1}(\rho) - \left(\frac{v'_{pol}}{v_{eq}} \right)_{n-1} \Delta\rho_{n-1}, \quad (7)$$

with $\tilde{A}_0 = A(\rho)$, and $\Delta\rho_0 = 0$. Whenever $\Delta\rho \sim \rho$, higher order terms become important, although $\rho \gg \Delta\rho$ is automatically satisfied. Eq.(7) converges provided that the Cauchy condition

$$|\tilde{A}_n(\rho) - \tilde{A}_{n-1}(\rho)| \ll \epsilon \quad (8)$$

is satisfied for an arbitrarily small ϵ . We shall see below how to integrate the corrected asymmetry through the star so as to estimate the accumulated effect along the whole propagation of the non-spherical flame.

2.1 Correction Term of the Asymmetry

The correction term for the asymmetry (Eq. 6), contains a derivative of the polar speed with respect to the density, and therefore, we need to know the dependence of the laminar

¹ The fractal velocity, v_{frac} , increases with the density, in Eq. (1), because the minimum scale l_{min} decreases faster with density than the laminar velocity, v_{lam} (see Paper I).

² It can be checked that the Lipschitz condition is satisfied by the function $\tilde{A}(\Delta\rho)$.

speed with the density and composition of the fuel in order to calculate the correction term. In this subsection we calculate the correction term for C+O progenitors. Using the interpolation formulae given by Woosley (1986); Timmes & Woosley (1992); and Arnett (1996), we find

$$v_{lam} = 92 \times 10^5 \left(\frac{\rho}{2 \times 10^9} \right)^{0.805} \left[\frac{X(^{12}\text{C})}{0.5} \right]^{0.889} \text{ cm s}^{-1}, \quad (9)$$

which is approximately³ valid in the density range $0.01 \leq \rho_9 \leq 10$. In the particular case in which $d = 2.5$ ⁴, the effective polar speed v_{pol} (see Eq. 1) does not depend on the laminar speed v_{lam} , so that we could say that v_{pol} is to some extent “independent of the microphysics”⁵

$$v_{pol}(\rho_u) = 0.282 \rho_u^{0.8} \left(\frac{g L_{max} \delta \rho}{\rho_u^{2.6}} \right)^{0.5} \text{ cm s}^{-1}. \quad (10)$$

Here, $\delta \rho = \rho_u - \rho_b$ is the density jump at the flame, i.e., the difference between burned (ρ_b) and unburned (ρ_u) material densities. We note that this is, in general, different from the the density difference between the polar and equatorial fronts $\Delta \rho = \rho_{eq} - \rho_{pol}$ (see Eqs. 3 - 7). Thus

$$\frac{\partial v_{pol}}{\partial \rho_u} = \frac{0.225 \left(\frac{g L_{max} \delta \rho}{\rho_u^{2.6}} \right)^{0.5}}{\rho_u^{0.2}} - \frac{0.141 \rho_u^{2.1} \left(\frac{2.6 g L_{max} \delta \rho}{\rho_u^{3.6}} + \frac{g L_{max}}{\rho_u^{2.6}} \right)}{(g L_{max} \delta \rho)^{0.5}}. \quad (11)$$

Using Eqs. (1) and (9), it is possible to obtain the polar fractal speed, v_{pol} , for any C+O composition with an arbitrary fractal dimension d

$$v_{pol} = 14.1683 (0.208752)^d X(^{12}\text{C})^{0.889} \times \quad (12)$$

³ We should note that equation (9) is only approximate and it is used for simplicity reasons, more realistic results could probably be obtained directly interpolating the velocities given in table (3) of Timmes & Woosley 1992, and will be addressed in future calculations.

⁴ This is actually the maximum fractal dimension estimated in Paper I.

⁵ In fact, recent numerical simulations of supernovae have shown that the hydrodynamics of the explosion is independent of the microphysics of the flame (Gamezo et al. 2002). In paper I, we found that the minimum relevant hydrodynamic scale for the flame was $l_{min} \sim 10^5$ cm (for $\rho \sim 10^9$ g cm⁻³), and the flame evolution was “independent of the microphysics” since $l_{min} \gg \delta_f$ almost all the way, where δ_f is the flame width. We here stop the numerical integration when $l_{min} \sim \delta_f$ or $l_{min} \sim 20 \times \delta_f$ (see below). In the particular case that $d = 2.5$, using the fractal scaling given by eq. (1) we recover the independence with microphysics which was obtained through dimensional arguments by Khokhlov (1995), and is also consistent with laboratory results of Taylor (see Kull 1991). In this case, the flame does not depend directly on quantities, such as, the laminar velocity or the thermometric conductivity.

$$\rho_u^{0.8} \left[\frac{g L_{max} \delta \rho}{X(^{12}\text{C})^{1.778} \rho_u^{2.6}} \right]^{d-2}.$$

And, in general, the correction term is given by

$$\frac{1}{v_{eq}} \frac{\partial v_{pol}}{\partial \rho_u} \Delta \rho = \frac{1}{v_{eq} g^2 L_{max}^2 \delta \rho^3} \left[22.6693 \times (0.208752)^d X(^{12}\text{C})^{4.445} \left(\frac{g L_{max} \delta \rho}{X(^{12}\text{C})^{1.778} \rho_b^{2.6}} \right)^d \times \left(-1.625 (d - 2.30769) \rho_u \rho_b^5 + (d - 2.5) \rho_b^6 \right) \right] \Delta \rho ; \quad (13)$$

where, the value of $\Delta \rho$ must be calculated numerically (see the next section).

3 INTEGRATED ASYMMETRY

In order to compute the total asymmetry for a given set of initial conditions for the progenitor, we must integrate the following equations along both the equatorial and polar directions, respectively

$$\frac{dr_{eq}}{dt} = v_{eq}(\rho, t) \quad (14)$$

$$\frac{dr_{pol}}{dt} = v_{pol}(\rho, t) \quad (15)$$

where $v_{pol}(\rho) = \tilde{A}(\rho) v_{eq}(\rho)$, and v_{eq} is given by:

$$v_{eq} = v_{lam} \left(\frac{L_{max}}{l_{eq}} \right)^{(d-2)}. \quad (16)$$

where $l_{eq} = l_{min}$ at the magnetic equator of the star (Paper I):

$$l_{eq} = \frac{8\pi \left(\frac{B^2}{8\pi} + \frac{1}{2} \rho v_{lam}^2 \right)}{g \delta \rho}, \quad (17)$$

The equations above can be integrated simultaneously in one dimension outward through the star along with Eqs. (7) and (8) to give the integrated asymmetry $A_{tot}(\rho) = r_{pol}(\rho)/r_{eq}(\rho)$, up to a shell of density ρ . The integration of Eq. (14) is straightforward, while Eq. (15) is non-linear since the value of \tilde{A} depends on the actual position of the polar front r_{pol} . It is solved using the same iterative algorithm that gives the *corrected asymmetry* described in the previous section.

Until now, we have neglected the fact that the flame is actually propagating in an expanding star and have thus partially decoupled the equations of the burning front from the hydrodynamical motions of the full star. Since actual deflagrations are subsonic, the star will pre-expand ahead of the flame, and this will, in turn, affect the burning itself (see Figure 1).

To a very good approximation, we can assume an *homologous* expansion of the white dwarf and this allows a simple description of the expansion as a function of time, in

which the radius of the n -th zone at a given time t evolves according to

$$r_n(t) = a(t) r_n^o, \quad (18)$$

where r_n^o gives the distance to the center in the initial condition (i.e., in hydrostatic equilibrium), and $a(t)$ is the homology factor satisfying $a(0) = 1$. The density will then evolve according to

$$\rho_n(t) = \rho_n^o / a^3(t), \quad (19)$$

where ρ_n^o is the density at the n -th zone in hydrostatic equilibrium, so that in the comoving frame of each zone the density will decrease with time.⁶

It is easy to see that the stellar expansion should produce a slower flame front than in the stationary case. This is due to the fact that when the deflagration reaches the radius r^n , the density there will be lower than it is without expansion. Therefore, the propagation velocity will be modified accordingly. The distance between zones is now $dr'_{eq} = a(t) dr_{eq}$, and $dr'_{pol} = a(t) dr_{pol}$, for each of the propagation directions. The n -th zones evolve according to

$$r_{eq'_n} = r_{eq'_{n-1}} + dr_{eq'_{n-1}},$$

and

$$r_{pol'_n} = r_{pol'_{n-1}} + dr_{pol'_{n-1}},$$

respectively.

We have computed the total asymmetry by taking into account the stellar expansion effect upon the density, for different initial chemical compositions of the white dwarf progenitor. We have integrated Eqs. (14) and (15) together with Eqs. (18) and (19), using a subroutine to interpolate step by step the physical properties of the deflagration front, i.e., the laminar velocity and the density jump, and the value of the magnetic field. We have employed an analytical function for $a(t)$, namely $a(t) = 0.25t + 1$ obtained from a numerical fit to the homologous expansion solutions of Goldreich & Weber (1980). The magnetic field strength has been assumed to decrease approximately linearly with the radial coordinate (see Wendell et al. 1987, and Paper I), and the initial density and gravity of the progenitor are depicted in Figures 2 and 3, respectively, as functions of the stellar radius. To compute the variation of the magnetic field in the comoving frame of the flame, we have assumed magnetic flux conservation. The computed progenitor models were resolved in 10^3 zones, giving a physical resolution ~ 1.5 km for a star with a radius $R = 10^5$ km. The integration was stopped when the polar combustion front reached a shell with density $\rho \sim 10^7$ g cm⁻³ for which the transition to detonation is believed to occur (Khokhlov 1995). This is a first step towards a more

⁶ We note that some deviation of a perfect homologous expansion should be expected mainly due to the fact that, as the flame is accelerated downstream under the action of hydrodynamical instabilities, shock and pressure waves may travel ahead of the flame and disturb locally the stellar structure. Nonetheless, since the deflagration evolves under approximate isobaric conditions, the actual expansion is expected to be nearly close to the homology assumed here.

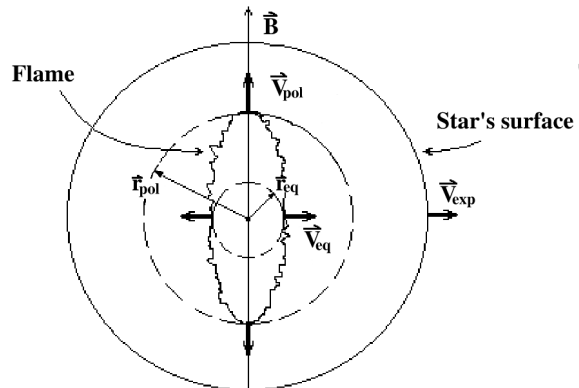


Figure 1. Schematic representation of the propagation of the front inside a white dwarf. Here \vec{B} indicates the direction of the dipolar magnetic field, \vec{V}_{exp} is the star's expansion velocity, \vec{V}_{pol} and \vec{V}_{eq} are the fractal polar and equatorial velocities, and r_{pol} and r_{eq} are the polar and equatorial radii, respectively, as described in the text. We note that the combustion is isobaric to a very good approximation, and the density jump in the flame is $\sim 10^{-1}$ times the density value.

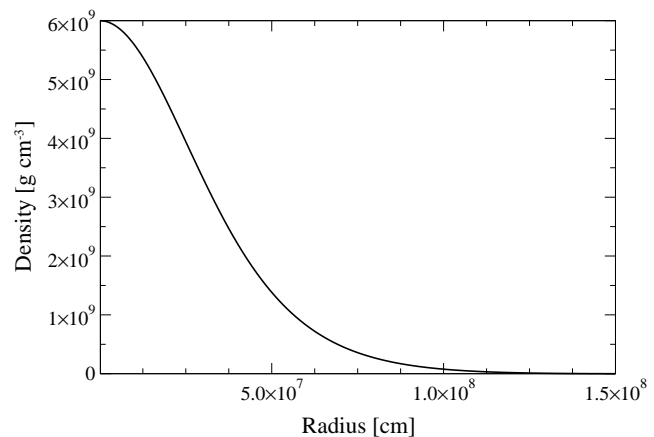


Figure 2. Initial density of the white dwarf progenitor as a function of the stellar radius.

complete calculation, but nevertheless contains all the essential ingredients necessary to address the total asymmetry A'_{tot} , namely

$$A'_{tot} = r'_{pol} / r'_{eq}, \quad (20)$$

where, generally speaking, $r'_{eq} > r_{eq}$ and $r'_{pol} > r_{pol}$.

4 RESULTS

The results of the calculations are shown in Figures 4 to 8. The instantaneous asymmetry near the stellar surface (for a density $\rho = 5 \times 10^7$ g cm⁻³) is shown in Figure 4 for several progenitors with C-O compositions as a function of the surface magnetic field.

Integrated asymmetries are depicted in Figure 5 for three different compositions (see captions) and a maximum

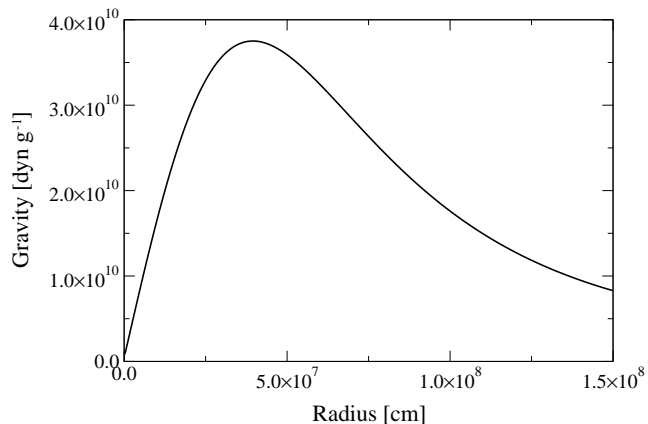


Figure 3. Initial absolute value of the gravity of the white dwarf progenitor as a function of the stellar radius calculated for a progenitor with an electron fraction $Y_e = 0.5$.

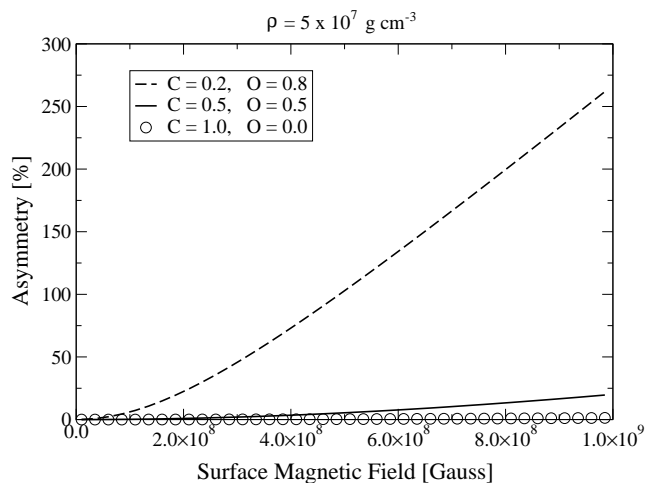


Figure 4. Instantaneous asymmetry for progenitors with different initial compositions [(a) $X(^{12}\text{C}) = 0.2$, $X(^{16}\text{O}) = 0.8$; (b) $X(^{12}\text{C}) = 0.5$, $X(^{16}\text{O}) = 0.5$; and (c) $X(^{12}\text{C}) = 1.0$, $X(^{16}\text{O}) = 0.0$] as a function of the magnetic field at a density $\rho = 5 \times 10^7 \text{ g cm}^{-3}$.

surface magnetic field $B = 10^9 \text{ G}$. It is apparent from Figs. 4 and 5 that heavier progenitors develop larger instantaneous asymmetries, but the lighter ones achieve the largest integrated asymmetries. Hence, it is important to understand the reasons behind such behavior for future applications.

The key aspect for this behavior may be traced back to saturation effects of the flame as follows. The value of l_{min} (see Eq. 17) indicates that it must decrease as the density decrease, but it clearly cannot be arbitrarily small. In fact, there is a minimum value associated with the width of the flame δ_f , which we will call the saturation scale, l_{sat} .

The asymmetry between the polar and equatorial directions begins to decrease when the instabilities in the polar front reach the saturation limit l_{sat} . The polar front will then

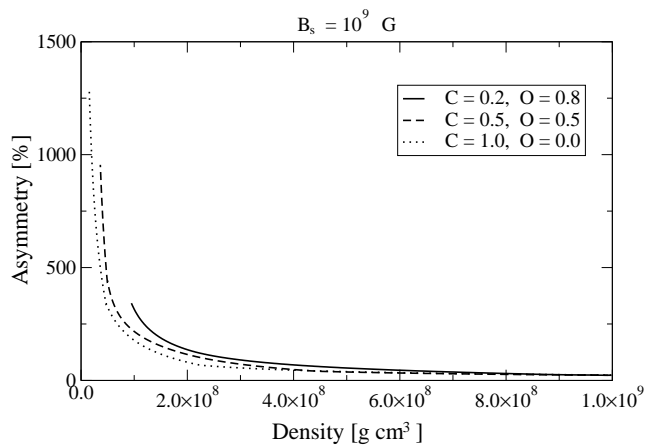


Figure 5. Integrated asymmetries for the progenitors (a) $X(^{12}\text{C}) = 0.2$, $X(^{16}\text{O}) = 0.8$; (b) $X(^{12}\text{C}) = 0.5$, $X(^{16}\text{O}) = 0.5$; (c) $X(^{12}\text{C}) = 1.0$, $X(^{16}\text{O}) = 0.0$. A surface field $B = 10^9 \text{ G}$ is assumed for all cases (which corresponds to a core $B \approx 10^{10} \text{ G}$), and a saturation scale of $20 \delta_f$. Taking lower values for the saturation scale higher integrated asymmetries are obtained. A general trend of the asymmetry effect is seen here, i.e., lighter progenitors show higher integrated asymmetry (while heavier progenitors have higher instantaneous asymmetry, for a given density and magnetic field, as shown in Fig. 4). This graph can be also interpreted as a display of the evolution history of the asymmetry. In the beginning, when the flame is still propagating in a high density medium, the asymmetry is very low. Later on, near the end of the deflagration regime, the asymmetry largely increases until the front encounters very low densities and the flame vanishes.

stop accelerating, while the equatorial front will be still accelerating. This will give place to a symmetrization phase that will last until the flame is quenched, or a transition to detonation occurs. We cannot predict exactly this symmetrization effect here, but if a transition to detonation occurs at densities $\sim 10^7 \text{ g cm}^{-3}$, then the errors in our present calculation must be small. On the other hand, if no transition to detonation takes place, then the uncertainties in our estimates will depend upon the density at which the flame quenches and will be as large as small the density is. Due to the same reason, we predict smaller symmetrization effects on lighter progenitors, i.e., progenitors with $X(^{12}\text{C}) = 0.5$ and $X(^{16}\text{O}) = 0.5$ will reach the saturation limit later on at lower densities, and will, therefore, develop larger integrated asymmetries (see Fig. 5).

It is known that if $l_{sat} = l_{min} \sim \delta_f$ thermodiffusive effects must be taken into account and, in fact, in most of the laboratory flames $l_{sat} \geq 20 \delta_f$ is observed (see Bychkov et al. 1999). Since no definitive answer to this question exists, we have calculated the integrated asymmetry for different values of the saturation scale between these two extremes (i.e., from $l_{sat} = \delta_f$ to $20 \delta_f$) in Figure 6, for the progenitor (a) of Figure 5. In Figure 7, we have fixed the saturation scale at $l_{sat} = 20 \delta_f$, in order to compare the integrated and the instantaneous asymmetry variations with the surface magnetic field for the same progenitor. Analysing these figures, we find that the integrated asymmetry is enormous if $l_{sat} \sim \delta_f$, and can be larger than 1000% if the magnetic

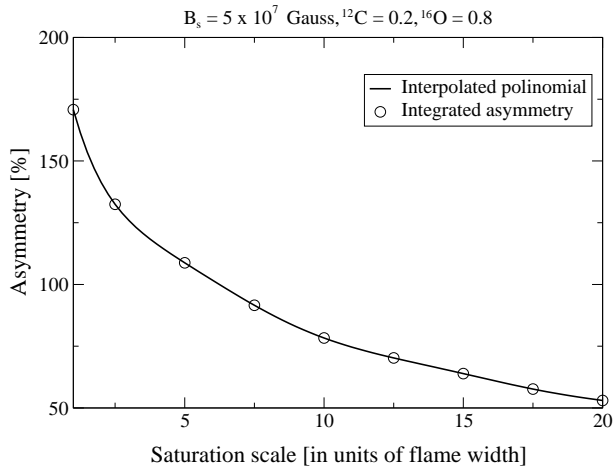


Figure 6. Integrated asymmetry vs saturation scale l_{sat} in units of the flame width δ_f , for the progenitor (a) of Figure 5 with chemical composition $X(^{12}\text{C}) = 0.2$, $X(^{16}\text{O}) = 0.8$. A surface field $B = 5 \times 10^7$ G is assumed.

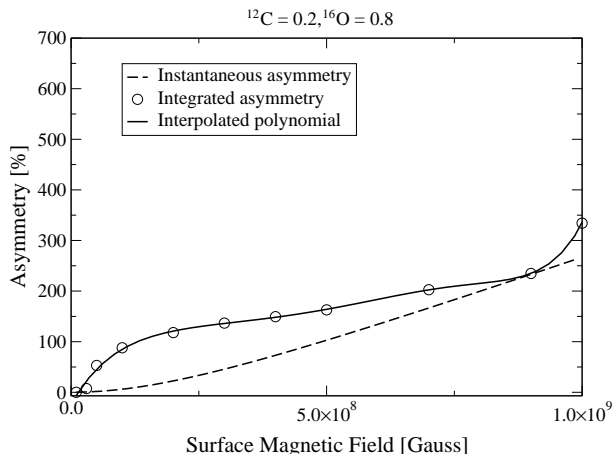


Figure 7. Circles - Integrated asymmetry vs surface magnetic field strength for the progenitor with chemical composition $X(^{12}\text{C}) = 0.2$, $X(^{16}\text{O}) = 0.8$, and a saturation scale $l_{sat} = 20 \delta_f$; Full line - seven-degree polynomial curve that fits the numerical results; Dashed line - instantaneous asymmetry for the same progenitor at a (surface) density $\rho \sim 10^7$ g cm $^{-3}$.

field is $\gtrsim 10^9$ G. When $l_{sat} \sim 20 \delta_f$ is imposed, the asymmetries are smaller but can be still very large, for instance, the progenitor shows a maximum asymmetry of the order of 350% for $B = 10^9$ G (Fig. 7). When the field is reduced to 5×10^7 G, the asymmetry drops. In this case, it presents a total asymmetry of $\sim 50\%$, for $l_{sat} \sim 20 \delta_f$ (Figure 8), which is in the ballpark of what polarimetric observations suggest ($\sim 20\%$ or less, see the next section; Leonard et al. 2000, Wang et al. 1997, Howell et al. 2001).

5 DISCUSSION AND CONCLUSIONS

It has been generally assumed that supernovae explosions are spherical. However, recent polarimetric studies of several supernovae have revealed intrinsic linear polarization that

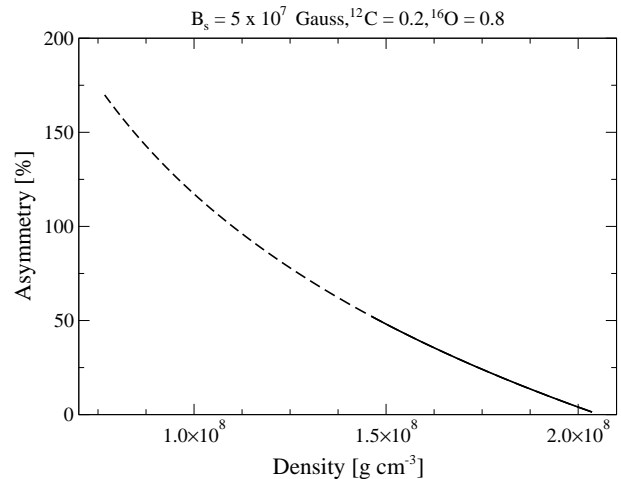


Figure 8. Integrated asymmetries for progenitor (a) $X(^{12}\text{C}) = 0.2$, $X(^{16}\text{O}) = 0.8$, with a surface field $B = 5 \times 10^7$ G, and saturation scales $l_{sat} = \delta_f$ (dashed line), and $20 \delta_f$ (full line). This represents the set of parameters that better fits observational data from SN Ia spectropolarimetric studies and experimental knowledge from laboratory flames. We have stopped the calculations when the flame vanishes. At this time, expansion can start symmetrizing the flame, although more efficient symmetrization must be expected during the coasting phase of the remnant due to enhanced turbulent diffusion.

seems to be evidence of asymmetric explosion (see Branch et al. 2001; Leonard et al. 2000; Howell et al. 2001). In the present work, we have investigated the effects of the magnetic field of the white dwarf (WD) progenitor on the propagation of the burning front of thermonuclear supernovae, and found that an asymmetry develops that could, in principle, help to explain observed asymmetries in these systems.

The magnetic field strengths inferred for isolated WDs are between 3×10^4 G and 10^9 G, while for WDs in AM Her binaries, they are in the range 10^7 G to 2×10^8 G (Wickamasinghe & Ferrario 2000) and could be further amplified by compression during the accretion phase (Cumming 2002). Magnetic fields had not been taken into account in previous studies of thermonuclear supernovae because their pressure is found to be much smaller than the gas pressure. Nonetheless, our studies have revealed that the magnetic fields act upon the hydrodynamical instabilities that develop in the flame front (where the magnetic pressure is larger than the ram pressure; see Eq. 2) and quench their growth in the direction perpendicular to the field lines. As a consequence, an *asymmetry* develops between the magnetic polar and equatorial axis that gives a prolate shape to the burning front.

We should emphasize that our analysis of the Rayleigh-Taylor mode interactions at the flame front has been based on the model described by Zeldovich et al. (1966, 1980)⁷, and its results are in qualitative agreement with 2-D and 3-

⁷ The Zeldovich et al.'s model for the mode-mode interactions of burned cells explains the saturation of the exponential growth of the hydrodynamic instabilities and gives the lower cut-off assumed for the instability which depends mainly on the saturation scale as explained above (see Eq. 17 above and also Eq. 4 of Paper I).

D numerical studies of the Rayleigh-Taylor (R-T) instability development in fully turbulent magnetized layers without combustion (see, Jun, Norman & Stone 1995, and references therein), and with numerical simulations of thermonuclear flames in 2D and 3D (see Khokhlov 1995). Jun et al.'s results, actually reveal a tendency, in the nonlinear regime, for an increase of the growth rate of the Rayleigh-Taylor instabilities in the direction parallel to the magnetic field lines (the polar direction), which would amplify the asymmetry effect here investigated, and an inhibition of the growth rate in the direction perpendicular to the magnetic field lines (equatorial direction) like in the present investigation.

The calculations performed in the former sections show that the integrated asymmetry in the velocity fields may be very large if the surface magnetic fields are near a maximum value ($\sim 10^9$ G). Observed asymmetries are much less extreme. At least three alternatives to solve this mismatch come to mind. The first is that white dwarfs in binary systems, which are thought to be the progenitors of SNIa supernovae, never have magnetic fields of such an intensity. Since pre-supernova systems samples are highly incomplete, it is difficult to address the likelihood of this conjecture (see below). The second possibility is that asymmetries do not develop that much because the saturation scale $l_{sat} \gg 20 \delta_f$ in these systems. This possibility cannot be totally disregarded since the saturation scale may be substantially different in these systems from that obtained in laboratory deflagration fronts. The third way out would be that even if the explosion itself could be largely asymmetric, the observed remnant could be efficiently symmetrized in the very early phases of the expansion. Nevertheless, it would be worth to search for a subset of very asymmetric remnants, perhaps not even identified as such because a jet-like morphology has never been expected.

On the other hand, if the surface magnetic field is reduced to more moderate values ($\lesssim 5 \times 10^7$ G), we have found that the total asymmetry drops (for saturation scales $\sim 20 \delta_f$) to a value of $\sim 50\%$ which is much more in agreement with the asymmetries inferred from present observations. For instance, for the type Ia supernova 1999by, the first clear example of an object of that class with asymmetric structure, an intrinsic polarization of $\sim 0.8\%$ was observed that was interpreted as produced by radiation from an oblate or prolate distribution of scattering electrons with an asymmetry between 17% and 50%, depending on the inclination of the object relative to the line of sight (Howell et al. 2001). Another important aspect to be noted is that in SN1999by, Si lines stronger than in normal type Ia SNe have been detected. This could be explained, in the framework of our model, as a result of an incomplete burning in the equatorial direction followed by a smaller production of Ni which, in turn, could explain the observed redder light curve. Yet another possibility may be that the prolate flame produces a transition to detonation first on the polar direction, thus disrupting the star before the equatorial direction had the chance to reach the requirements for detonation transition, therefore resulting in an incomplete burning and smaller Ni production.

So far, only $\sim 15\%$ of the type Ia supernovae have been examined through polarimetric observations and they do not present, in general, high polarization degrees. The model here described, could, in principle, explain the asymmetry

inferred from these spectropolarimetric observations, if the fraction of strongly magnetized white dwarfs (WD) is not too large. In fact, it seems that only 5% of the isolated white dwarfs are magnetized, but this figure increases to 25% in binary systems.

Very recently, Cumming (2002) has suggested that due to an effect of screening and magnetic field amplification in rapidly accreting systems, an asymmetry (due to magnetic field effects) can be more likely observed in super-soft X-ray binaries. This constitutes a new (and separate) observational constraint to the study and detection of the asymmetry effect presented here. In fact, the search of asymmetric SNIAs in super-soft X-ray binaries could be an easier task than to survey a full sample of very young type Ia supernova remnants through spectropolarimetric observations.

In the model proposed here, if higher expansion coefficients, $a(t)$, were considered, then either a higher magnetic field strength or a lower saturation scale would be needed in order to produce the same value for the total asymmetry. In other words, we are not able to establish completely a set of parameters for the model, and a statistically significant sample of asymmetric type Ia SNe would be required for that purpose. It must be also pointed out that in a real explosion, $a(t)$ should assume a distinct functional dependence on the pole and the equator, and this would enhance the asymmetry effect. In the model presented here, there is, in fact, a spherical symmetric remnant surrounding a prolate flame.

We have assumed in the model a constant fractal dimension all over the explosion. This approximation is justified by the very fast growth of the instabilities in the thermonuclear front, so that the turbulent regime is achieved well before an appreciable expansion of the star.

Finally, we should mention that other models have been suggested in the literature to explain the asymmetries in type Ia supernovae explosions, although all of them have their problems (see e.g., Howell et al 2001). The model here investigated also presents limitations that could, at least in part, be solved with the help of future multidimensional numerical calculations and larger samples of observed asymmetric astrophysical objects. Laboratory experiments of the deflagration of mixtures of gases in the presence of magnetic fields could also provide alternative tests of the asymmetry effect in the flame front and also of the fractal model examined. The configuration of these experiments must be settled carefully in order to ensure the growth of the R-T instability over a wide spectrum of perturbations, and the geometry of the apparatus must be chosen in such a way that its minimum size is larger than the minimum wavelength of the perturbations (Ghezzi 2002).⁸

ACKNOWLEDGEMENTS

We acknowledge partial support of the Brazilian Foundations FAPESP (São Paulo) and CNPq to this work.

⁸ We are of course supposing that the fractal model can explain the turbulent regime of a supernova flame. Previous laboratory experiments (Gostintsev et al 1988) and numerical simulations of fractal flames in the wrinkled regime (Filyand et al. 1994; Blinnikov et al. 1996) seem to support this hypothesis.

REFERENCES

- Arnett, W. D., *Supernovae and Nucleosynthesis*, Princeton University Press (1996).
- Blinnikov, S. I., & Sasorov, P. V., *Phys. Rev. E*, **53**, 5, (1996).
- Bychkov, V. V., Kovalev, K. A., & Liberman, M. A., *Phys. Rev. E*, **60**, 3, 2897, (1999).
- Chandrasekhar, S., *HYDRODYNAMIC AND HYDROMAGNETIC STABILITY*, **Dover** (1981).
- Chandrasekhar, S., & Fermi, E., *ApJ*, **118**, 116 (1953).
- Chanmugam, G., *Annu. Rev. Astron. Astrophys.*, **30**, 143-84 (1992).
- Cumming, A., *Mon. Not. R. Astron. Soc.*, **333**, 3, 589-602 (2002).
- Crank, J., & Nicolson, P., *Proc. Cambridge Phil. Soc.*, **43**, 50 (1947).
- Filyand, L., Sivashinsky, G. I., & Frankel, M., *Physica D*, **72**, 110 (1994).
- Gamezo, V. N., Khokhlov, A. M., & Oran, E., *American Astronomical Society Meeting*, **200**, # 14.01 (2002).
- Ghezzi, C. R., PhD thesis, University of São Paulo, Brasil (2002).
- Ghezzi, C. R., de Gouveia Dal Pino, E. M., & Horvath, J. E., *ApJ*, **548**, L193-L196 (2001).
- Goldreich, P., & Weber, S. V., *ApJ*, **238**, 991-997 (1980).
- Gostintsev, Yu., A., Istratov, A., G., & Shulenin, Yu., V., *Combustion Explosions and Shock Waves*, **24**, 70 (1988).
- Howell, D. A., Höflich, P., Wang, L., & Wheeler, J. C., *ApJ*, **556**, 302 (2001).
- Jun, B., Norman, M. L., & Stone, J. M., *ApJ*, **453**, 332 (1995).
- Khokhlov, A., *ApJ*, **449**, 695 (1995).
- Kull, H. J., *Physics Report*, **206**, 5, 197-325 (1991).
- Leonard, D. C., Filippenko, A. V., & Matheson, T., 2000, *AIP Conf. Proc.*, **522**, *Cosmic Explosions*, ed. S. S. Holt & W. W. Zhang (melville: AIP), astro-ph/9912337.
- Niemeyer, J. C., & Hillebrandt, W., *ApJ*, **452**, 769 (1995).
- Niemeyer, J. C., & Woosley, S. E., *ApJ*, **475**, 740-753 (1997).
- Timmes, F. X., *ApJ*, **390**, L107 (1992).
- Timmes F. X., & Woosley, S. E., *ApJ*, **396**, 649-667 (1992).
- Wang, L., Wheeler, J., C., & Höflich, P., *ApJ*, **476**, L27-L30 (1997).
- Wendell, C. E., Van Horn, H. M., & Sargent, D., *ApJ*, **313**, 284, (1987).
- Wickamasinghe, D. T., & Ferrario, L., *PASP*, **112**, 773, 873-924 (2000)
- Woosley, S. E., 1986, *Nucleosynthesis and Chemical Evolution*, ed. B. Hauck, A. Maeder, & G. Meynet, 1 (Geneva: Swiss Society of Astrophysics and Astronomy, Geneva Observatory).
- Woosley, S. E., in *Supernovae*, ed. A. G. Petschek, 1990, 182, (New York: Springer-Verlag).
- Zeldovich, Ya. B., *J. Appl. Mech. & Tech. Phys.*, **7**, 68 (1966).
- Zeldovich, Ya. B., Barenblatt, G. I., Librovich, V. B., & Makhviladze, G. M., "The Mathematical Theory of Combustion and Explosions", **New York: Plenum** (1985).
- Zeldovich, Ya. B., Istratov, A. G., Kidin, N. I., & Librovich, V. B., 1980, *Combustion Sci. Technol.*, **24**, 1.

This paper has been typeset from a $\text{\TeX}/\text{\LaTeX}$ file prepared by the author.